
An Article Submitted to

INTERNATIONAL JOURNAL OF
CHEMICAL REACTOR ENGINEERING

**Influence of Free Stream Turbulence
Intensity on Heat Transfer and Flow
Around Four In-Line Elliptic Cylinders in
Cross Flow**

Ramadan Y. Sakr*

Nabil M. Berbish[†]

Ali A. Abd-Aziz[‡]

*Shoubra Faculty of Engineering, Benha University, Egypt, rsakr85@yahoo.com

[†]Benha University, Egypt, n11264@yahoo.com

[‡]Benha University, Egypt, alymech@yahoo.com

Influence of Free Stream Turbulence Intensity on Heat Transfer and Flow Around Four In-Line Elliptic Cylinders in Cross Flow

Ramadan Y. Sakr Dr., Nabil M. Berbish Dr., and Ali A. Abd-Aziz

Abstract

Effect of free stream turbulence intensity on heat transfer and flow characteristics around four in-line elliptic cylinders in cross flow was experimentally and numerically investigated. The elliptic cylinders examined had an axis ratio (b/c) of (1:3), with zero angle of attack (major axis is horizontal) and they were heated under constant heat flux condition. Three different sizes of free stream turbulence producing grid (screen) inserted 300 mm upstream the test cylinders are used to study the effect of the free stream turbulence. The turbulence intensities levels of 5.6%, 8.3% and 10.5% are obtained from the grid sizes. The effect of cylinder spacing ratio (L/c) were examined within Reynolds number (based on free stream velocity and major axis length) ranged from 3640 to 66240. It was observed that the local and average Nusselt numbers of the tested elliptic cylinders increase with increasing the free stream turbulence intensity. The results showed that the maximum enhancement ratio for the average Nusselt number (average Nusselt number of the tested cylinder with grid/ average Nusselt number of a single elliptic cylinder without grid) was found to be about 1.93, and was obtained for the second elliptic cylinder in four in-line cylinders at $L/c=1.5$, $Re=6150$ with free stream turbulence intensity of 10.5%. Also, the flow characteristics were varied drastically with varying both the longitudinal spacing ratio and the inserted grid (screen). Moreover, an empirical correlation for the average Nusselt number of the second elliptic cylinder of four in-line cylinders was obtained as function of Reynolds number and free stream turbulence intensity.

KEYWORDS: Free stream turbulence, Turbulence intensity, In-line arrangement, Four elliptic cylinders, Cross flow

1. INTRODUCTION

The exploration of compact and high-performance heat exchanger for conserving energy is a very important and urgent problem. Heat exchangers made of tubes of circular cross section are commonly used in industry. However, flow over these tubes is not always perpendicular to the tube axis which makes the tube cross-section in the direction of flow to have an elliptic shape. In general, the elliptic tube geometry can represent the circular tube and can also represent a very thin plate depending on the value of the axis ratio. Moreover, it is found that their drag coefficient at small angles of attack is lower than that of a circular cylinder. This may be an advantage feature when using elliptic tubes as a heat transfer surface element, since the pumping power needed for fluids to flow around them may become very small and the heat exchanger may be more compact [1-4].

The literature on forced convection heat transfer from elliptic cylinders without grid (screen) showed a good number of investigations. The first measurements of the local heat transfer coefficient were reported by Seban and Drake [5] and by Drake et al. [6]. Who investigated their experimental studies for cylinders of axis ratio of 1:4 and 1:3, respectively at small angles of attack (0° , 5° , and 6° only). Ota et al. [7] performed experimentally forced convection from elliptic cylinder of axis ratio 1:3, placed in a uniform stream of air in the Reynolds number ranged from 8000 to 79000 and for angles of attack varying from 0° to 90° . The angle of attack was found to have a strong influence on the overall heat transfer enhancement ratio. Nishiyama et al. [2] conducted experimentally forced convective heat transfer from elliptic cylinders of axis ratio 1:2, placed in tandem arrangements. The study was performed for four cylinders at various values of Reynolds number ranged from about 15000 to 70000.

Badr [8] studied numerically forced convection heat transfer from a single elliptic cylinder. It was found that, the maximum Nusselt number occurs at zero angle of attack and small axis ratio. Khan et al. [9] investigated experimentally forced convection cross flow heat transfer of hot air over an array of in-line elliptical tubes carrying cold water. It was found that the Nusselt number and hence, the heat transfer rate, increased with increasing both water and air Reynolds numbers. Abdel Aziz et al. [4, 10] carried out experimental and numerical studies on heat transfer and flow characteristics around a single elliptic cylinder, two elliptic cylinders in-line, and three staggered cylinders in cross flow of air. It was found that, the average Nusselt number for the downstream cylinder was higher by about 15-84% than that of the single elliptic cylinder, depending on the cylinders arrangement and spacing ratios. Berbish [11] investigated experimentally and numerically forced convection heat transfer and flow around four staggered elliptic cylinders in cross flow of air. The results showed that the maximum average Nusselt number enhancement ratio for the downstream elliptic

cylinder in four staggered cylinders was found to be about 2.0, and was obtained for spacing ratios of $S_x/c=2.5$, $S_y/b=2.5$ at $Re=32000$.

The effect of free stream turbulence on heat transfer coefficient at a surface of a plate is reviewed by Kandjuyan et al. [12]. The influence of free stream turbulence on the heat transfer from circular cylinders in cross flow has formed the subject of numerous experimental investigations, but few works have performed for elliptic tubes. For example, the influence of turbulence intensity on heat transfer from elliptic cylinder has been performed by Seban [13], the axis ratio of the cylinder was 1:4 and $56000 < Re < 236000$. His results indicate that the local heat transfer increase with the free stream turbulence intensity. However, Seban did not measure the turbulence intensity and gave only the characteristics of the grids that are used to promote turbulence. The combined effect of free stream turbulence and tunnel blockage on average Nusselt numbers of circular cylinders was reviewed by Morgan [14]. The influence of turbulence intensity on heat transfer coefficient of circular cylinders was investigated by Dyban and Epick [15], Dyban et al. [16], and Lowery and Vachom [17]. These works demonstrate that the heat transfer coefficient increases with turbulence intensity and that this effect is more intense when the Reynolds number is higher. For a circular cylinder in a cross flow of high turbulence intensity, Simmons et al. [18] and Ching and O'Brien [19] have reported fluctuations in heat transfer from measurements in the stagnation region of the cylinder. However, no measurements were reported for other locations on the cylinder circumference.

Haung et al. [20] conducted experiments to investigate the effects of free stream turbulence and unsteady wake on conductive heat transfer coefficient of a heated cylinder.

They found that the higher wake passing frequency produces more frequent velocity fluctuations, more broad velocity profiles, and a storage degree of turbulence intensity which are caused by the upstream wake generator and turbulence grid to enhance heat transfer. Terekhov et al. [21] studied experimentally the hydrodynamic features of the gas flows past a rib and past a downward step in characteristics separation-flow regime, and distribution of pressures, temperatures and heat transfer coefficients behind obstacles in such flows are presented. They also examined the effect of enhanced external turbulence on thermal and dynamic characteristics of the separated flows. The effects of turbulence integral length scale and turbulence intensity on the convective heat transfer rate from a heated circular cylinder were investigated experimentally by Sak et al. [22]. Tests were conducted at a Reynolds number of 27700, relative turbulence intensity ranges from 2.9% to 8.3% and turbulence integral length scale to cylinder diameter ranges from 0.5 to 1.47. They found for integral length scale of 0.78 heat transfer increases with the increase of turbulence intensity and for turbulence intensity of 6.9% heat transfer rate decreased with

increasing turbulence length scale. The effect of free stream turbulence on heat transfer and pressure coefficients of a turbine blade was investigated in low Reynolds number flow by Choi et al. [23]. Cascade inlet Reynolds number based on blade chord length was varied from 15700 to 105000 and turbulence intensity was varied from 0.68% to 15.31%. Their study documents the effect on increasing Reynolds number and free stream turbulence in suppressing separation, promoting boundary layer transition, and enhancing heat transfer on blade surface.

Kondjoyan and Daudin [24] performed experimentally the effects of free stream turbulence intensity on heat and mass transfer at the surface of a circular cylinder and an elliptical cylinder, axis ratio 1:4. It was found that the influence of the elliptical cylinder ratio on the mean transfer coefficients values was much less than the effect of the air flow properties. Also, the local heat transfer coefficient is much higher at the stagnation point of an elliptical cylinder than elsewhere at the surface. Scholten and Murray [25, 26] investigated experimentally unsteady heat transfer and velocity of a cylinder in cross flow with low and high free stream turbulence. It is observed that, the level of heat transfer fluctuations for the high turbulence tests is higher in the region where the turbulent boundary layer exists, but it is lower in the wake region at the very back of the cylinder. This local region of low heat transfer fluctuations is a consequence of less mixing of the fluid within the wake region due to the narrower wake associated with delayed separation of the boundary layer. Ahmed and Badr [27] investigated numerically heat transfer from an inclined elliptic tube in a convective environment with fluctuations in the free stream including the effect of buoyancy forces. It was found that the time average of the Nusselt number was increased with increasing amplitude of the fluctuations and with decreasing frequency.

The influence of free stream turbulence on heat transfer and flow around elliptic cylinders is not studied extensively. Therefore, the main purpose of the present study is to clarify the heat transfer coefficients and flow behavior around four in-line elliptic cylinders in cross flow, with different values of free stream turbulence intensity. The tested elliptic cylinders having an axis ratio 1:3 and they are placed in-line arrangement with zero angle of attack. Moreover, the effects of Reynolds number and longitudinal spacing ratio are examined.

2. EXPERIMENTAL SETUP, INSTRUMENTATIONS AND PROCEDURES

The experimental setup is a suction type wind tunnel, designed to give air flow across a heated horizontal elliptic cylinder in in-line arrangement with other three unheated elliptic cylinders. The heated elliptic cylinder may be placed at first, second, third or fourth in the in-line arrangement. The setup consists mainly of a centrifugal blower, air passage, test section, and measuring instruments as shown in Fig. (1). A centrifugal type air blower is driven by an alternating electric

current motor of 5.0 hp, is used to supply the required air flow. The air flow discharge is controlled at the outlet of the air blower by means of a variable area outlet gate. Various values of Reynolds number based on cylinder major axis length are utilized in the experiments which ranged from 3640 to 66250.

The working section of the wind tunnel is 200 mm wide, 200 mm height, and 1200 mm long. For clean tunnel (without grid), the working section free stream turbulence intensity at the centerline of the tunnel in potential core is about 1%. Air enters through a smooth bell-mouth to the test section, after which air passes through a transition duct ending with a circular section of 140 mm diameter. Air flows then through a straightener (honey comb) before reaching the orifice-meter. The elliptic cylinders examined have an axis ratio (b/c) of 1:3, the major axis length (c) being 45 mm and the span-wise length 200 mm (aspect ratio of 4.44). They were made of wood (high smooth surface) with the aid of an elliptic edge cutter tool. Heating of the downstream test cylinder was conducted by means of an electric current passed through a nickel-chrome tape of 0.2 mm thickness, 5 mm width and 16.5 Ω total resistance, which is wound helically around the tested elliptic cylinder with a pitch of 1 mm; this provided approximately the condition of constant heat flux. The details of the heating elliptic cylinder are indicated in Fig. (2).

Twenty-two copper-constantan thermocouples (0.4 mm wire diameter) are distributed circumferentially, embedded on the cylinder surface of the central section, and fixed at the back of the nickel-chrome heater tape to measure the surface temperature of the heated elliptic cylinder. To confirm a uniform temperature distribution, three thermocouples are installed at the two ends and at mid span of the tested cylinder to measure the axial temperature. Air temperature entering and leaving the test section are measured by using two thermocouples.

A digital thermometer with a minimum reading of 0.1°C is employed for all the temperature measurements. Openings are located in the two side walls of the test section in order to change the spacing ratios (L/c) to take values of 1.5, 2.5 and 4.0 respectively. The spacing (L/c), is defined as the ratio between stream-wise distance between two centers of the cylinders to the major axis of the elliptic cylinder. The cylinders are arranged with zero angle of attack (α), where the major axis is horizontal. Three grids of 40x40 mm, 30x30 mm, and 20x20 mm were used to get different free stream turbulence values as shown in Fig. (3). These grids were located normal to the flow at distance of 300 mm from the elliptic cylinders arrangement. Also, the grids are formed from wooden smooth bars of 9 mm diameters. These grids give free stream turbulence level of 5.6%, 8.3% and 10.5% respectively. The free stream turbulence is defined as a ratio of free stream root mean square value of stream-wise velocity fluctuations u_{rmso} to the free stream mean velocity U_o , $Tu = u_{\text{rmso}} / U_o$.

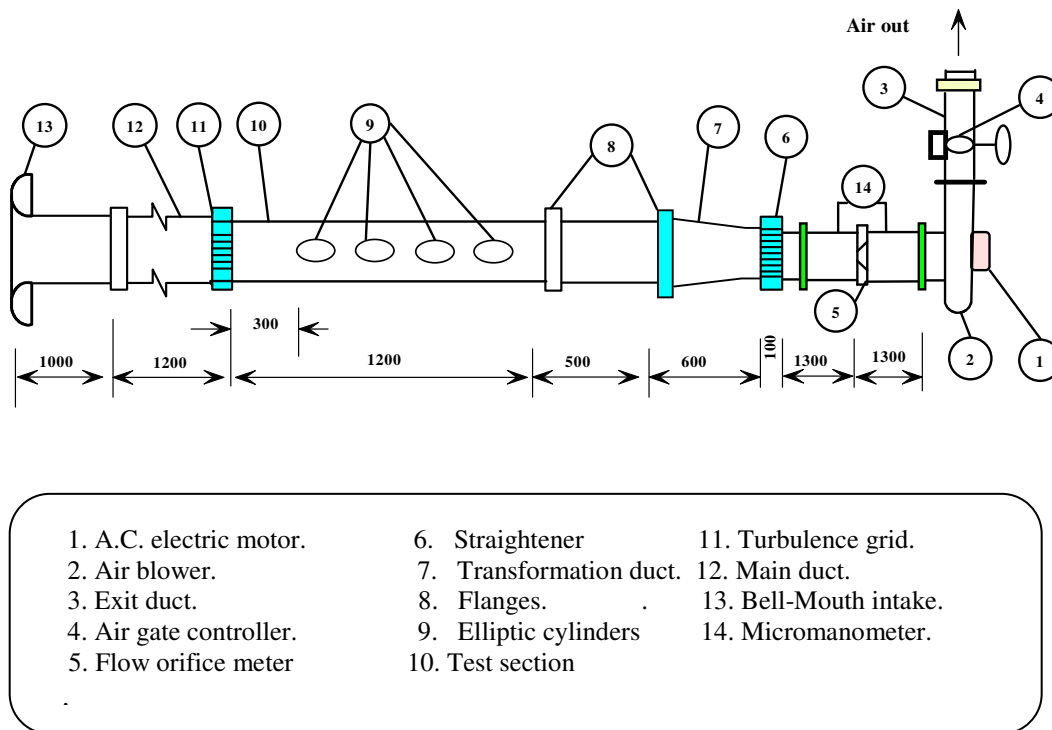


Fig. (1) The experimental setup

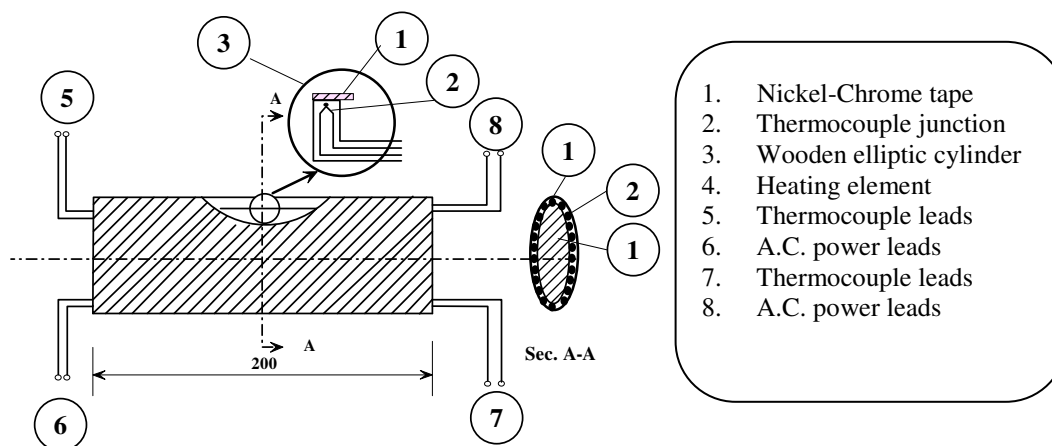


Fig. (2) Details of heated elliptical cylinder

The free stream mean velocity was measured at the centerline of the test duct using a Pitot tube connected to a micromanometer with a minimum reading of 10 Pa. The streamwise mean velocity and root mean square value of streamwise velocity fluctuations were measured with a Dantec 56C01 constant

temperature anemometer CTA with a Dantec 55P04 single-wire probe of 5 μm diameter platinum-plated tungsten wire. The hot wire probe has been mounted on a two-dimensional transverse mechanism of Dantec 56H100 model. The system is digitally controlled and easily interfaced to the computer and it allows recording of measured values. The measurements of the streamwise mean velocity and root mean square value of streamwise velocity fluctuations were carried out without heating, i.e. before the heat transfer measurements.

The input electric power is adjusted using a voltage regulator. It is calculated from the product of both the voltmeter and the ammeter readings. After steady state is achieved, the local heat transfer coefficient, h , and the corresponding local Nusselt number, Nu_x , are calculated, respectively, as follows:

$$h_x = \frac{q_w}{(T_x - T_{f,x})} \quad (1)$$

$$\text{Nu}_x = h_x c / K \quad (2)$$

where q_w , T_x , $T_{f,x}$, c , and K are the heat flux, local surface and film air temperatures, cylinder major axis length, and air thermal conductivity, respectively. The film temperature $T_{f,x}$ is calculated as: $T_{f,x} = 0.5(T_x + T_o)$.

Moreover, the average Nusselt number over the whole circumference of the elliptic cylinder, Nu_m , is calculated from integration of the local Nusselt number.

The uncertainty of the heat transfer coefficient or Nusselt number is estimated to be about $\pm 4.6\%$. Also, uncertainty of about $\pm 2.2\%$ is found in measuring the flow velocity or reported Reynolds number.

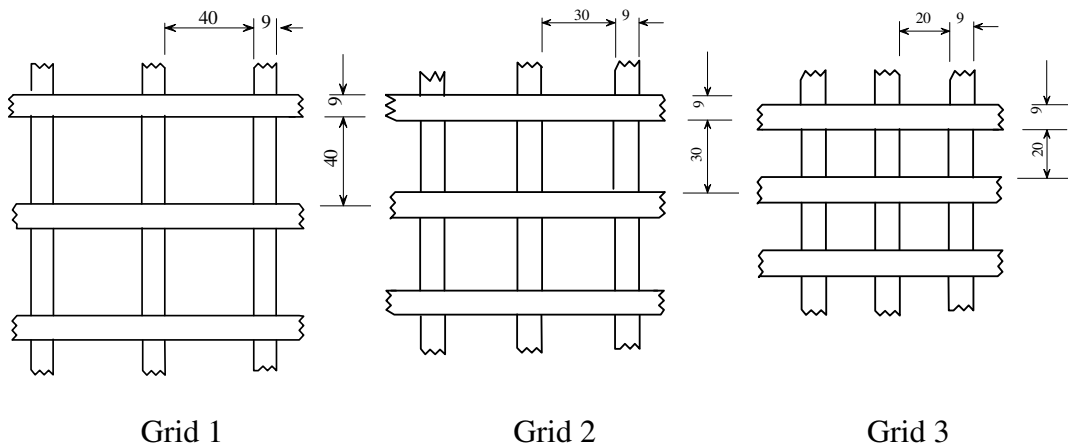


Fig. (3): Details of grids that producing free stream turbulence intensities

3. NUMERICAL APPROACH AND PROCEDURES

In the present experimental work, Reynolds number based on the major axis of the elliptic cylinder, c , ranges from 3640 to 66250. So, the flow can be considered turbulent flow. Turbulence is characterized by fluctuating quantities, e.g. velocity, temperature etc., the velocity fluctuations impact transport of quantities such as mass, momentum, and energy.

Direct simulation of all scales of velocity fluctuation is not computationally practical. Therefore, simplifications for turbulent flow solutions are necessary. Types of approaches for handling turbulent flows are through Reynolds averaging or filtering Navier Stokes equations. However, both methods introduce unknown terms into Navier Stokes equations; therefore, additional turbulence modeling is required to achieve the closure of the flow equations.

A number of different turbulence models can be applied when solving turbulent flow fields. The RNG k- ϵ (Renormalization Group theory) is selected for this analysis. The primary reasons for using the RNG k- ϵ turbulence model are that it allows for variation in the turbulent Prandtl number as a function of flow conditions, it provides a means for including low Reynolds number effects in the effective viscosity formulation, and it includes an extra, R_ϵ , in the ϵ equation to better model separated flows. The conservation equations for RNG k- ϵ turbulence model are given below, [28]:

k-turbulent kinetic energy:

$$\frac{\partial}{\partial t}(\rho k) + \frac{\partial}{\partial x_i}(\rho k u_i) = \frac{\partial}{\partial x_j} \left(\alpha_k \mu_{eff} \frac{\partial k}{\partial x_j} \right) + G_k + G_b - \rho \epsilon + -Y_M + S_k \quad (3)$$

ϵ -dissipation of turbulent kinetic energy:

$$\frac{\partial}{\partial t}(\rho \epsilon) + \frac{\partial}{\partial x_i}(\rho \epsilon u_i) = \frac{\partial}{\partial x_j} \left(\alpha_\epsilon \mu_{eff} \frac{\partial \epsilon}{\partial x_j} \right) + C_{1\epsilon}(G_k + C_{3\epsilon} G_b) - C_{2\epsilon} \rho \frac{\epsilon^2}{k} - R_\epsilon + S_\epsilon \quad (4)$$

Where:

$$G_k = -\rho u'_i u'_j \frac{\partial u_j}{\partial x_i}, \quad G_b = g_i \frac{\mu_t}{\rho Pr_t} \frac{\partial \rho}{\partial x_i}, \quad C_{3\epsilon} = \tanh \left| \frac{v}{u} \right|$$

$$R_\epsilon = \frac{C_\mu \rho \eta^3 (1 - \eta / \eta_o) \epsilon^2}{1 + \beta \eta^3} \frac{\epsilon^2}{k}, \quad \eta = \frac{S k}{\epsilon}$$

The G_k is the generation of turbulent kinetic energy due to mean velocity gradients, G_b is the generation of turbulent kinetic energy due to buoyancy, S_ϵ and S_k are user defined source terms, Y_M is the contribution of fluctuating dilatation to the dissipation rate and S is the modulus of the mean rate of strain tensor. The quantities α_k and α_ϵ are the inverse effective Prandtl numbers derived analytically by the RNG theory.

Turbulent viscosity

$$\mu_t = \rho C_\mu \frac{k^2}{\varepsilon} \quad (5)$$

The model constants $C_{1\varepsilon}$, $C_{2\varepsilon}$, α_k , α_ε , η_o , β , and C_μ in the above equations are as follows, (Fluent user manual, 2001):

$C_{1\varepsilon}=1.42$, $C_{2\varepsilon}=1.68$, $\alpha_k=\alpha_\varepsilon \approx 1.393$, $\eta_o=4.38$, $\beta=0.012$ and $C_\mu=0.0845$.

Fluent numerical code, version 6.2.16 is employed for all numerical simulations. Gambit 2.2.30 is used for the development of the computational grid.

The arrangement of the four elliptic cylinders and the computational domain are shown in Fig. (4). The computational domain resulted from the subtraction of the four elliptical cylinders sections from the rectangular duct section. The grid is made up of triangular elements to improve the quality of the numerical prediction near the curved surfaces. The number of finite volume faces ranges from 29700 to 42700 according to (L/c) is employed for the entire flow domain to attain grid independent solutions.

Finite volume discretization method is employed for solving the governing equations using a semi-implicit method for pressure linked equations, which is referred to as the SIMPLE procedure with segregated solver. To reduce numerical errors, second order upwind discretization schemes are used in the calculations. In Fluent code, there are four turbulence specification methods; (a) turbulence intensity and hydraulic diameter, (b) k and ε , (c) Turbulence intensity and length scale, and (d) turbulence intensity and turbulent viscosity ratio. In the present investigation the first method is used as it is recommended for flows downstream perforated plates or grids.

Each computational iteration, the governing equations are solved implicitly. The convergence of the computational solution is determined on scaled residuals for the continuity, energy equation and for many of the predicted variables. The total residual for a given variable is based on the imbalance in an equation for conservation of that variable summed over all computational cells. The settings for the scaled residuals for solution convergence are set to 10^{-3} for nearly all computed residuals. The only exception is the residual for the energy equation which is set 10^{-6} . The solution is considered to be converged when all of the scaled residuals are less than or equal to these default settings. Less than 400 iterations are generally needed for convergence.

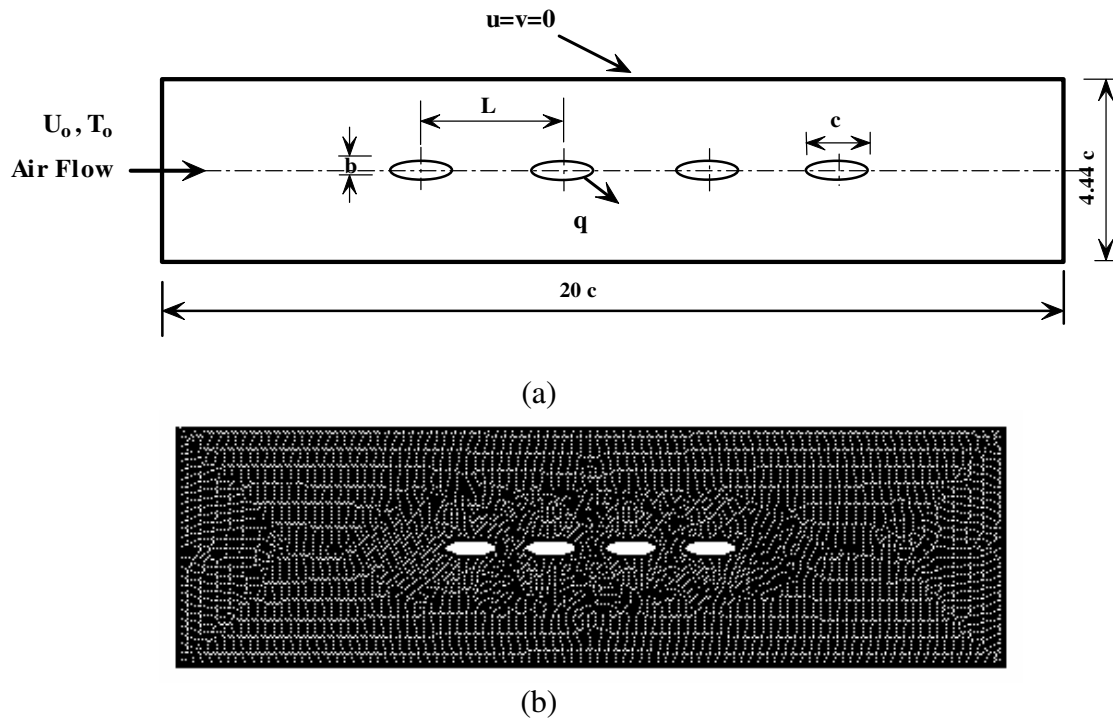


Fig. (4) Physical model and computational grid

4. EXPERIMENTAL RESULTS AND DISCUSSION

Heat transfer and flow around four in-line elliptical cylinders having an axis ratio (b/c) of 1:3 with zero angle of attack are investigated and explained within the range of Reynolds number (based on free stream velocity and major axis length) from 3640 to 66250. The effects of free stream turbulence intensity and cylinder spacing ratio are examined.

4.1. Local heat transfer results

The test heated elliptical cylinder may be placed at first, second, third or fourth in four cylinders in-line arrangement. Variation of local Nusselt number distributions around the whole circumference of the four elliptical cylinders with dimensionless surface path distance (S/c) are plotted without grids for different Reynolds numbers at various cylinder spacing (L/c) having values of 1.5, 2.5 and 4 in Figs. (5) – (16). The circumferential distance at upper (positive S) and lower (negative S) sides of the elliptical cylinder is extended along the abscissa in a non-dimensional path distance (S/c). At the smallest cylinder spacing ratio $L/c=1.5$, the local Nusselt number of the first cylinder reaches a maximum at the upstream stagnation point (leading edge) as shown in Fig. (5). Also, two shear layers are separated from the upstream cylinders and attached to the immediate downstream

cylinders. Then the Nusselt number attains maximum at the two attachment points on each cylinder.

The flow inside the wake region bounded by two neighboring cylinders and two separated shear layers is stagnant and thus the Nusselt number is low. Downstream of the attachment point, Nusselt number decreases with the surface distance due to the boundary layer development. Nusselt reaches a minimum near the separation point and then reaches a nearly constant value or increases slightly in the separated flow region, as indicated in Figs (6)-(8). At tested larger cylinder spacing ratio $L/c=2.5$ and 4.0 , a considerable variation of the local Nusselt number distribution occurs for the 2nd, 3rd, and 4th cylinders. That is, Nu attains a maximum at the leading edge, decreases with the surface distance, and reaches a minimum. Subsequently Nu increases slightly in the wake region as shown in Figs. (9)-(16). Such a drastic variation of Nu may be due to a change of the flow pattern around the 2nd, 3rd, and 4th cylinders. That is, the cylinder spacing is wide enough for the shear layers separated from the 1st, 2nd, and 3rd cylinders to roll up upstream of the 2nd, 3rd and 4th cylinders respectively. Accordingly, the main flow at the free stream temperature is entrained onto the front surface of the 2nd, 3rd, and 4th cylinders. Also, at $L/c=4.0$, it is observed that the profiles of Nu for all four cylinders are almost similar to those at $L/c=2.5$. Moreover, it is found that the local Nusselt number distribution for the first cylinder shows no essential variation with the cylinder spacing as presented in Figs. (5), (9), and (13).

However, the flow separates and the local Nusselt number reaches a minimum value close to $S/c=\pm 0.7$ independently of Reynolds number. Then reaches a nearly constant value upto $S/c=\pm 1.1$ for $Re \leq 21420$. At high Reynolds number ($Re \geq 31750$), the local Nusselt number begins to increase slightly downstream of the position of $S/c=\pm 0.8$, as indicated in Figs. (5)-(16). It may be reasonable to consider that the tested Reynolds number range is included within the subcritical flow regions, since the heat transfer distribution shows no essential change with Reynolds number [4, 7].

Three grids of different sizes 40x40, 30x30 and 20x20 mm are used for producing three free stream turbulence intensities of 5.6%, 8.3%, and 10.5% respectively. At $L/c=1.5$, the local Nusselt number distributions around the circumference of the second heated elliptic cylinder are plotted against the dimensionless surface path distance (S/c) at different Reynolds numbers and for the tested free stream turbulence values of 5.6%, 8.3% and 10.5%, as shown in Figs. (17), (18) and (19), respectively. The results show that the local Nusselt number is significantly increased with increasing the free stream turbulence intensities.

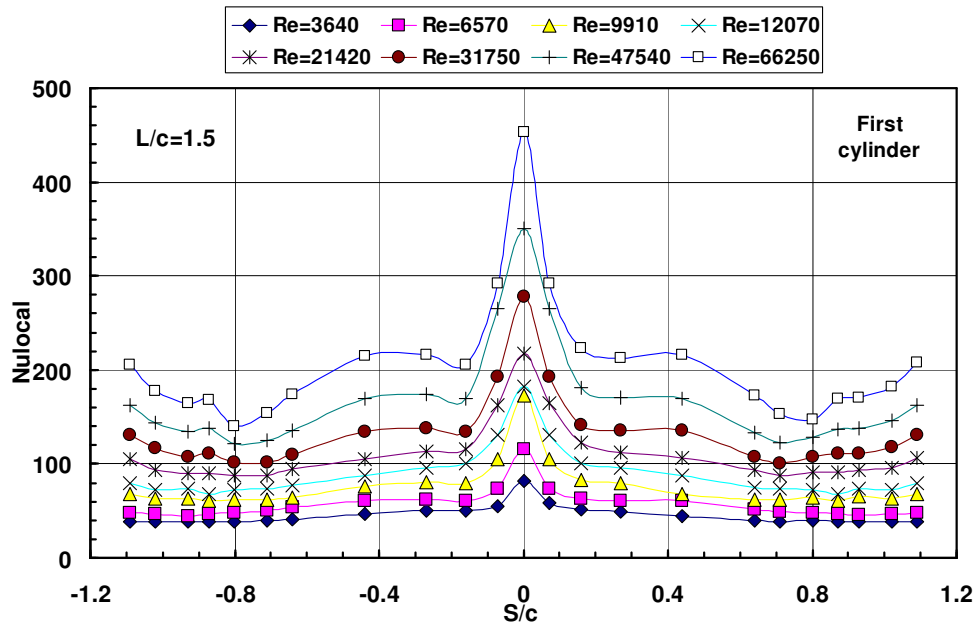


Fig. (5) Variation of local Nusselt number versus path distance (S/c) for first elliptic cylinder without grid at $L/c=1.5$

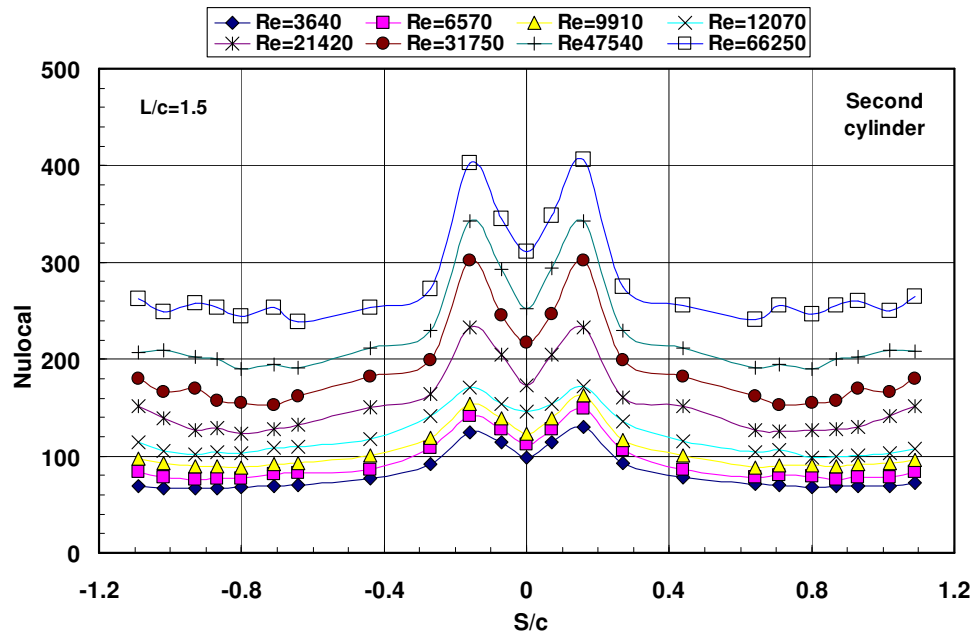


Fig. (6) Variation of local Nusselt number versus path distance (S/c) for second elliptic cylinder without grid at $L/c=1.5$

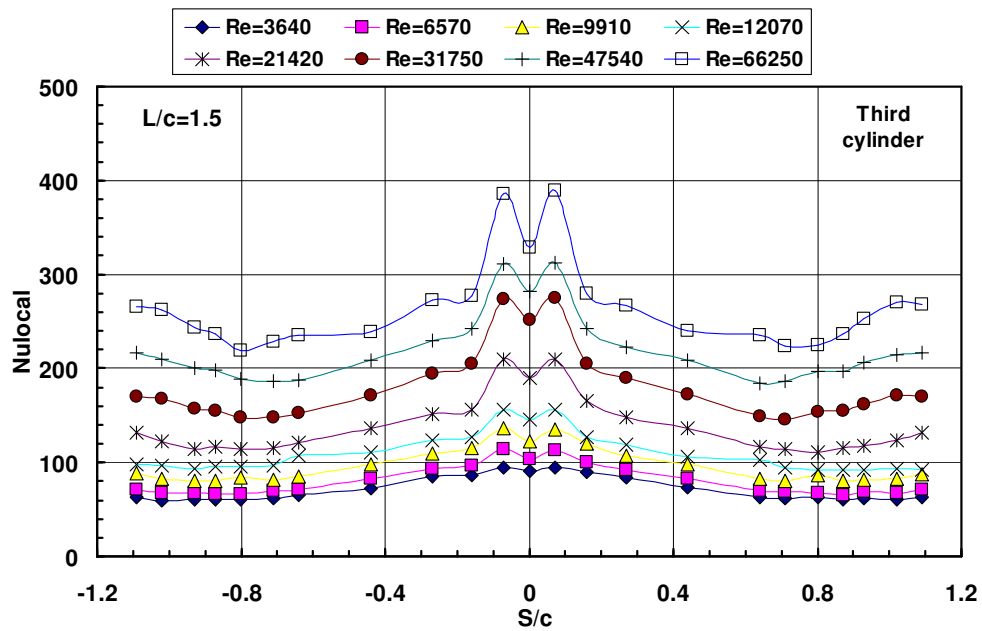


Fig. (7) Variation of local Nusselt number versus path distance (S/c) for third elliptic cylinder without grid at $L/c=1.5$

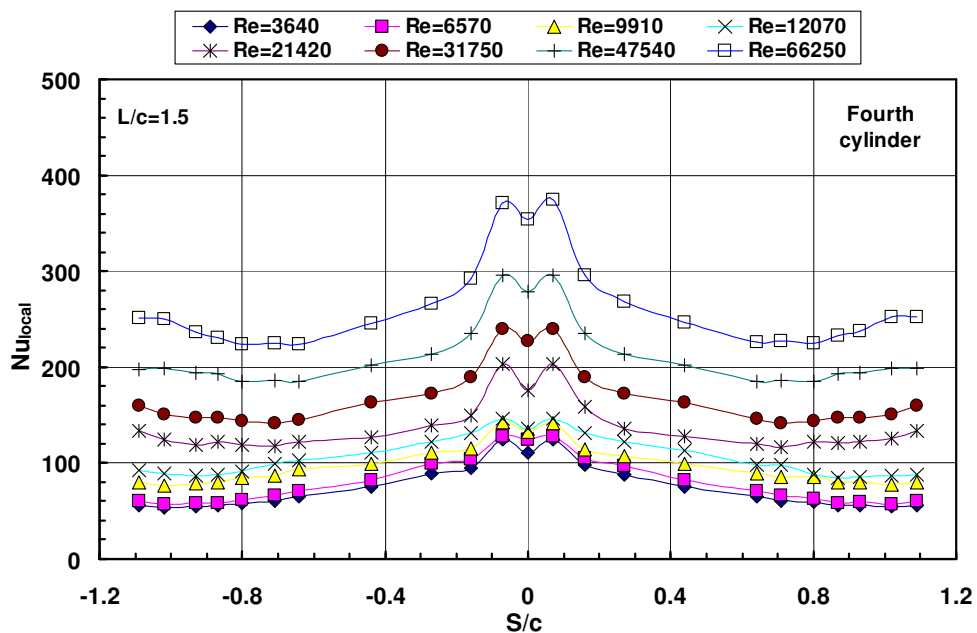


Fig. (8) Variation of local Nusselt number versus path distance (S/c) for fourth elliptic cylinder without grid at $L/c=1.5$

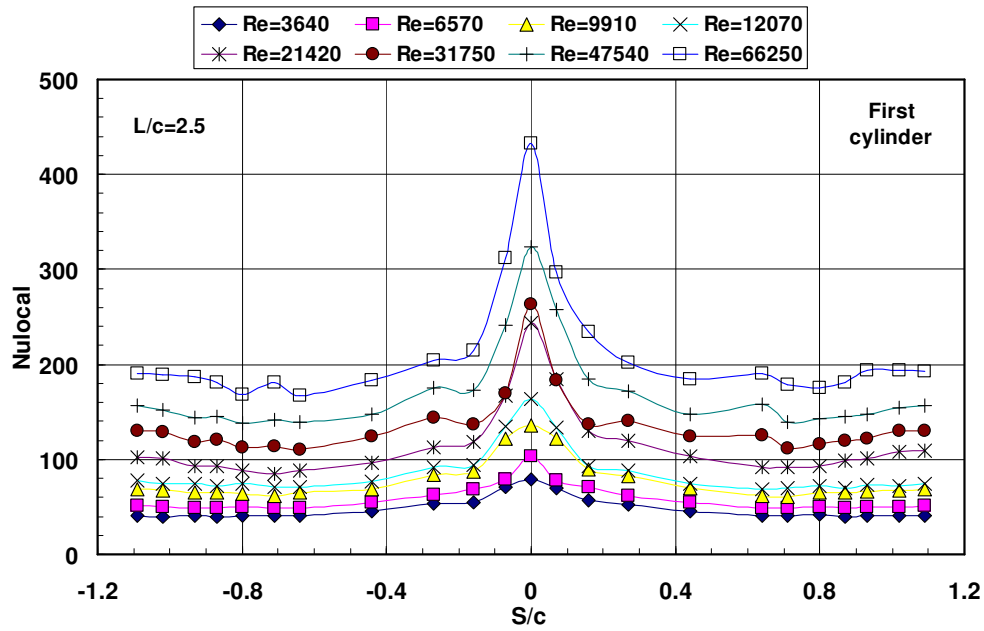


Fig. (9) Variation of local Nusselt number versus path distance (S/c) for first elliptic cylinder without grid at $L/c=2.5$

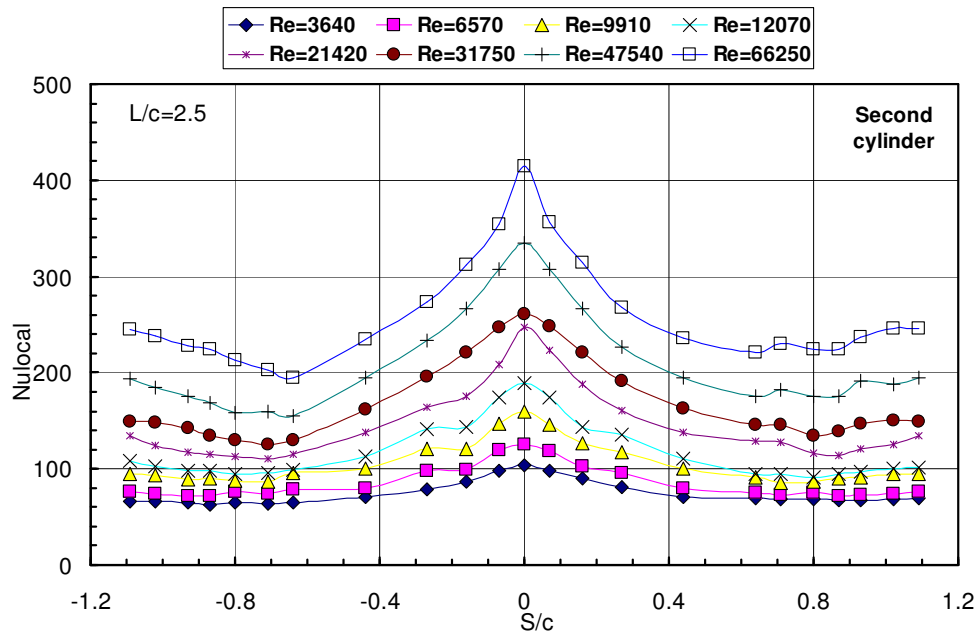


Fig. (10) Variation of local Nusselt number versus path distance (S/c) for second elliptic cylinder without grid at $L/c=2.5$

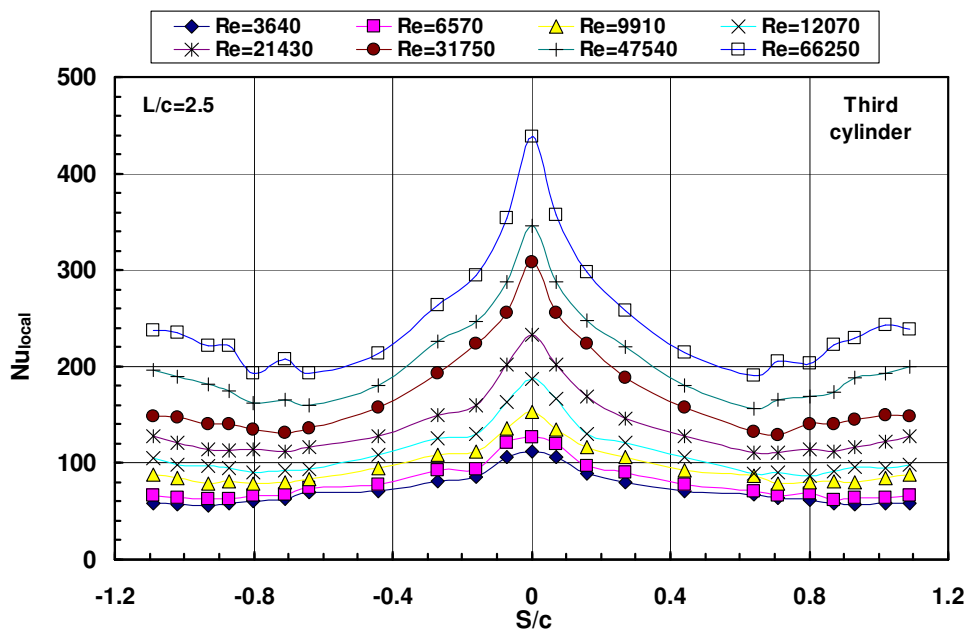


Fig. (11) Variation of local Nusselt number versus path distance (S/c) for third elliptic cylinder without grid at $L/c=2.5$

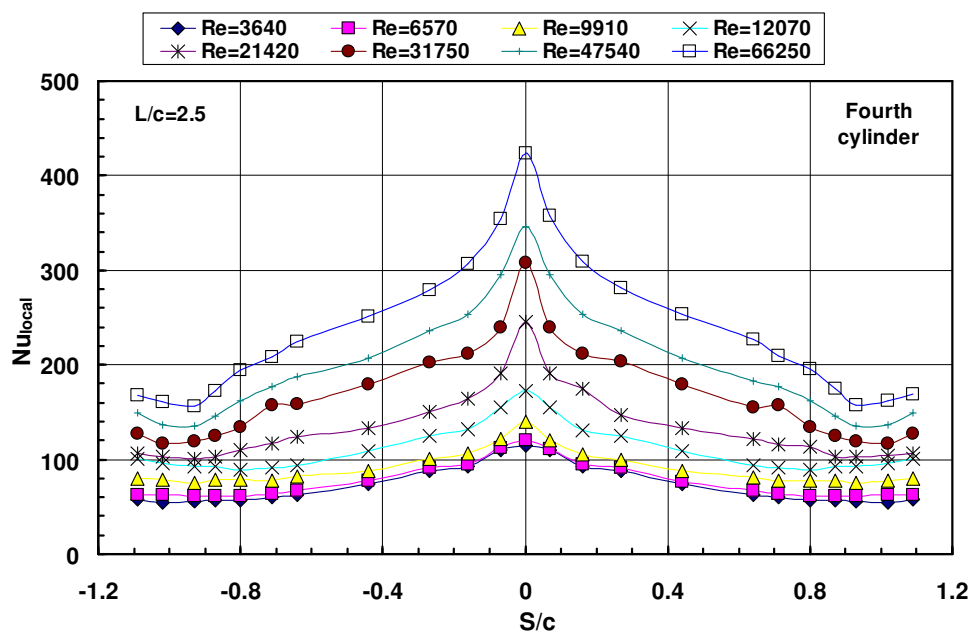


Fig. (12) Variation of local Nusselt number versus path distance (S/c) for fourth elliptic cylinder without grid at $L/c=2.5$

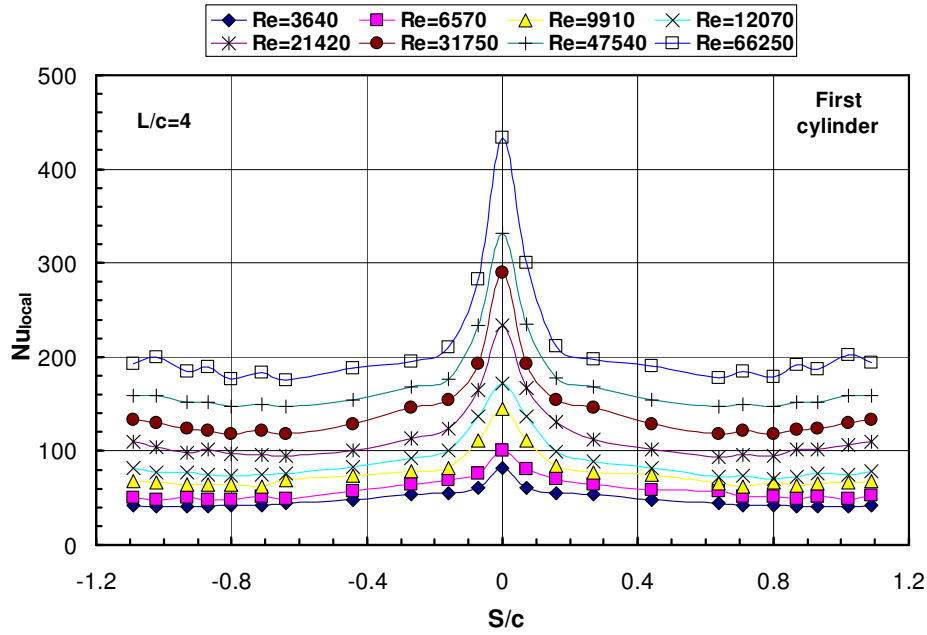


Fig. (13) Variation of local Nusselt number versus path distance (S/c) for first elliptic cylinder without grid at L/c=4.0

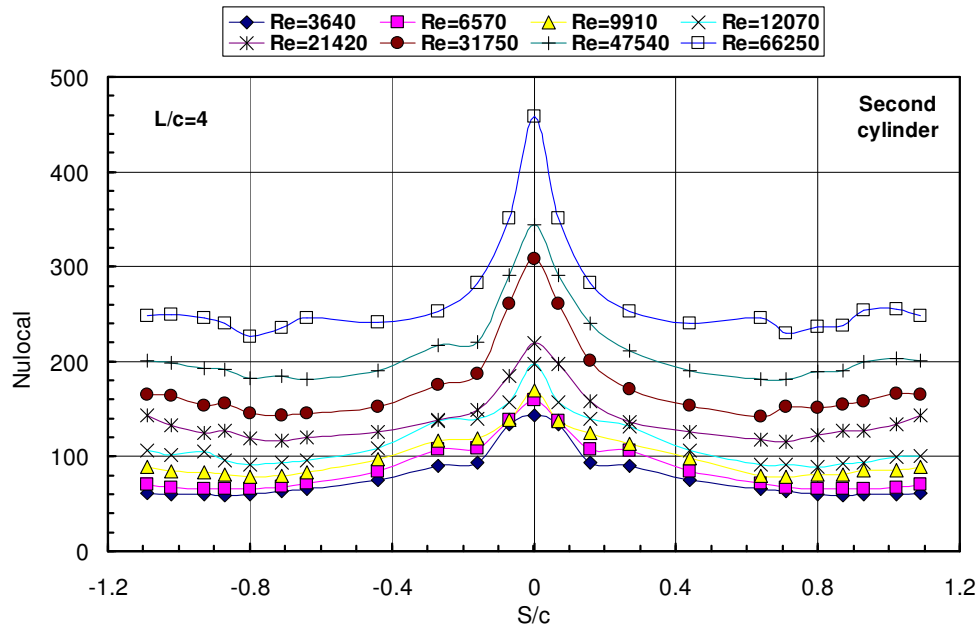


Fig. (14) Variation of local Nusselt number versus path distance (S/c) for second elliptic cylinder without grid at L/c=4.0

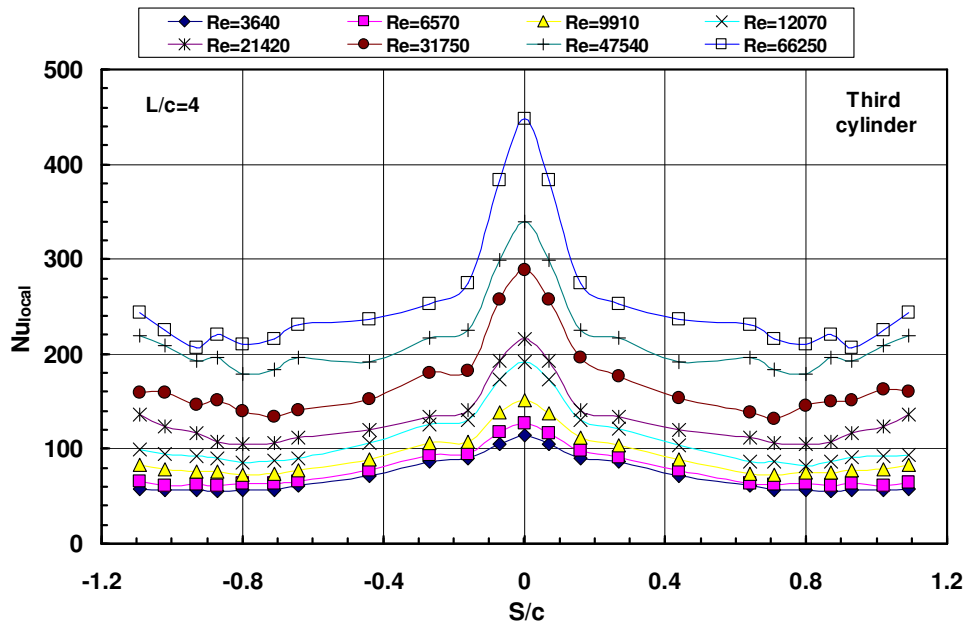


Fig. (15) Variation of local Nusselt number versus path distance (S/c) for third elliptic cylinder without grid at $L/c=4.0$

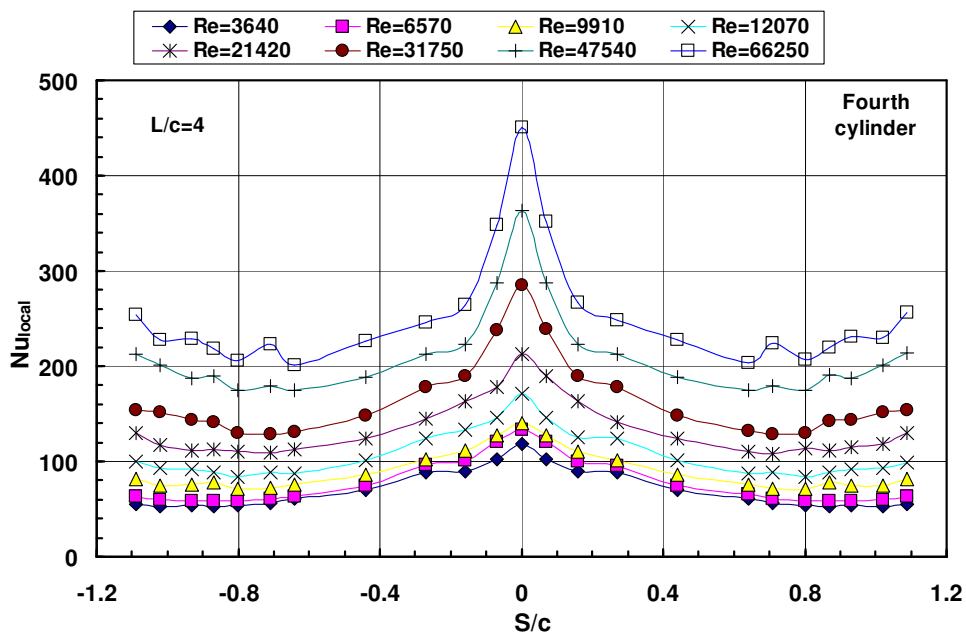


Fig. (16) Variation of local Nusselt number versus path distance (S/c) for fourth elliptic cylinder without grid at $L/c=4.0$

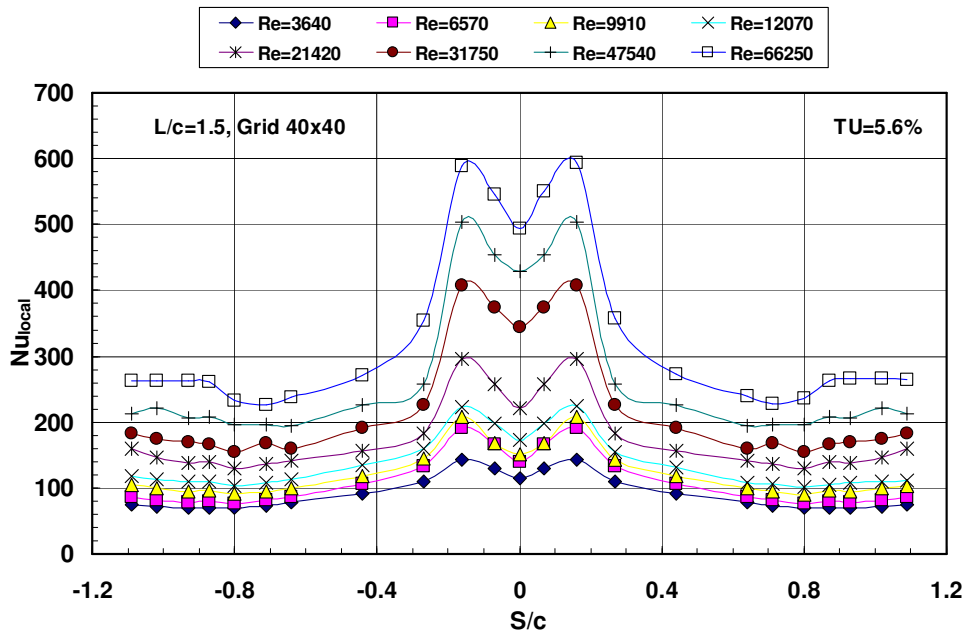


Fig. (17): Variation of local Nusselt number versus path distance (S/c) for second heated elliptic cylinder with grid 40x40 ($Tu=5.6\%$) at $L/c=1.5$

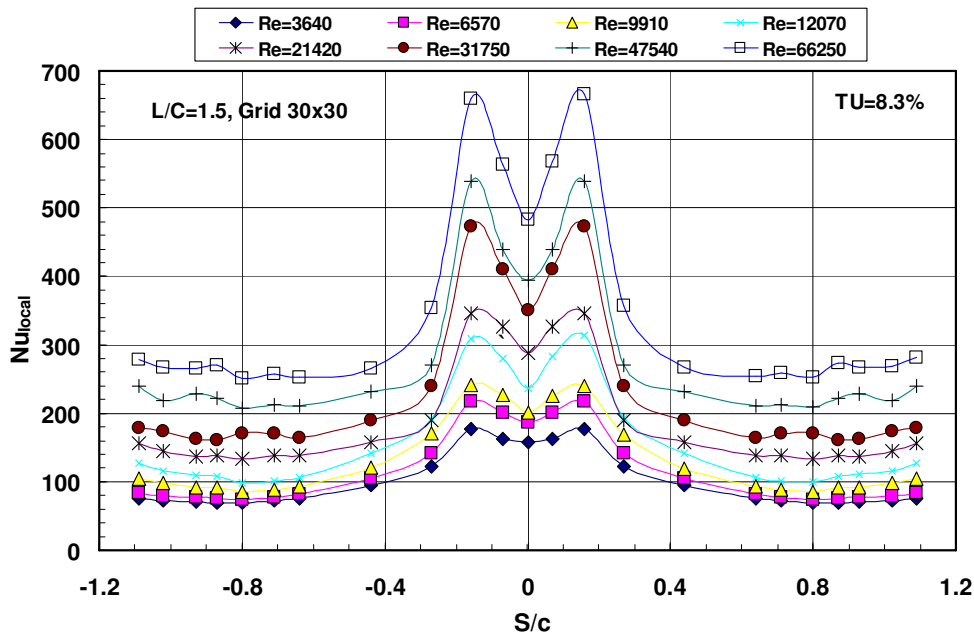


Fig. (18): Variation of local Nusselt number versus path distance (S/c) for second heated elliptic cylinder with grid 30x30 ($Tu=8.3\%$) at $L/c=1.5$

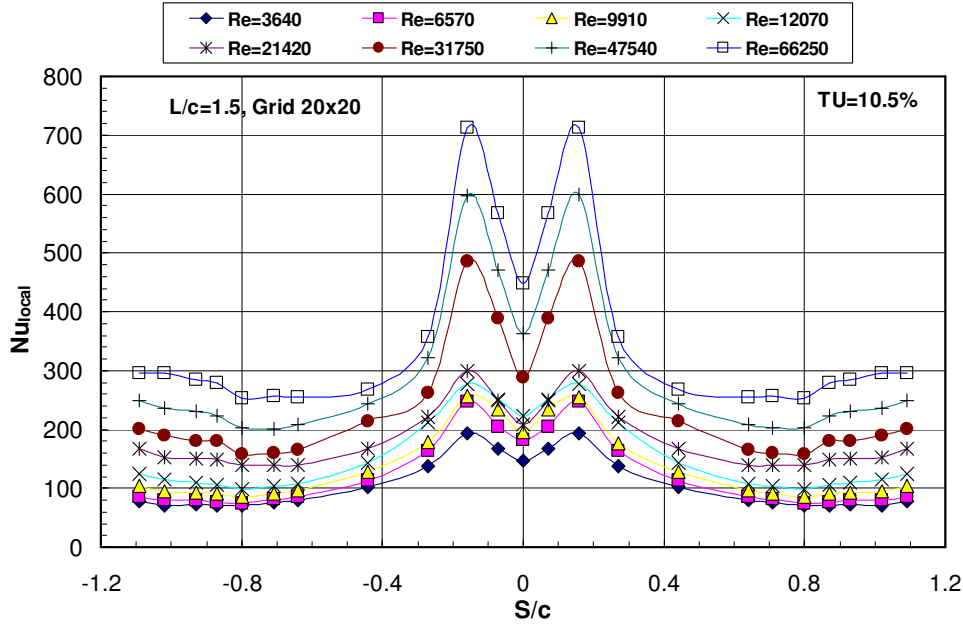


Fig. (19): Variation of local Nusselt number versus path distance (S/c) for second heated elliptic cylinder with grid 20×20 ($Tu=10.5\%$) at $L/c=1.5$

4.2. Average heat transfer results

A preliminary series of experiments for a single elliptic cylinder of axis ratio 1:3 with zero angle of attack without grid was conducted to check the accuracy of the experimental setup. The average Nusselt number for the single elliptic cylinder $Nu_{s,m}$ was correlated with Reynolds number, $Re=U_o c/v$, for $3640 \leq Re \leq 66250$ and the following correlation was obtained:

$$Nu_{s,m} = 0.612 Re^{0.528} \quad (6)$$

A comparison between the present correlation for a single elliptic cylinder, Eq. (6), and the correlation proposed by Ota et al. [7], and fair agreement was observed as shown in Fig. (20). Also, the figure illustrated that the results for the circular cylinder presented in [29] which has lower values than those for the elliptic tube. The comparison ensures the reliability and the validity of the present experimental setup and the methods of calculations.

The variation of the average Nusselt number for the heated second and fourth cylinders without grid versus Reynolds number at different cylinder spacing ratios are presented experimentally and numerically in Figs. (21)-(23) and are compared with the experimental results of four in-line cylinders obtained by Nishiyama et al. [2] and good agreement is obtained.

It can be observed that the average Nusselt number increases with increasing Reynolds number, due to the decrease in the boundary layer thickness and the strong mixing of fluid in the separated region. It is found that the average Nusselt number for the second cylinder is higher than that of the other tested cylinders for all tested spacing ratios. This may be attributed to that the 2nd cylinder is located in a highly turbulent and wide wake flow. The variation of the average Nusselt number of the 2nd cylinder versus Reynolds number at $L/c=1.5$ and for different free stream turbulence intensity values is illustrated experimentally and numerically in Fig. (24). Also, the figure shows the result of a single elliptic tube of axis ratio, $c/b=1:4$ at $Tu=11\%$ that obtained by [24]. It is observed from the figure that the results of ref [24] are lower than the present results for the 2nd heated elliptic cylinder and this may be attributed to the additional turbulence produced by the first cylinder in the present tube arrangement. Also, the results show that increasing trend for the average Nusselt number with the increase in the free-stream turbulence. The heat transfer enhancement (Nu_m with grids / Nu_m without grid) is about 10%, 14% and 16% for free stream turbulence of 5.6%, 8.3% and 10.5% respectively, as shown in Fig. (25). From Figs (24, 25), it is observed that the numerical predictions are in good agreement with the experimental results. It is concluded that, the maximum enhancement ratio for the average Nusselt number (average Nusselt number of the tested cylinder with grid/ average Nusselt number of a single elliptic cylinder without grid) is found to be about 1.93, and is obtained for the second elliptic cylinder in four in-line cylinders at $L/c=1.5$, $Re=6150$ with free stream turbulence intensity of 10.5%.

Moreover, empirical correlation for the average Nusselt number of the second elliptic cylinder in four in-line cylinders is obtained for $L/c=1.5$ as function of Reynolds number, and free stream turbulence intensity, and the following correlation is obtained:

$$Nu_m = 1.73 Re^{0.445} Tu^{0.089} \quad (7)$$

Where, the constant in the above equation are obtained by the least square method using the present measured data. The maximum deviation of the present data from Eq. (7) is about $\pm 10\%$ within the ranges of $3640 \leq Re \leq 66250$, $5.6 \leq Tu\% \leq 10.5$.

The velocity vectors for different spacing (L/c) values of 1.5, 2.5 and 4 at $Re=12070$ and $Re=47540$ respectively are illustrated in Fig. (26). The figure shows that only the second cylinder is subjected to highly turbulent flow region as a result of flow interaction of the first cylinder.

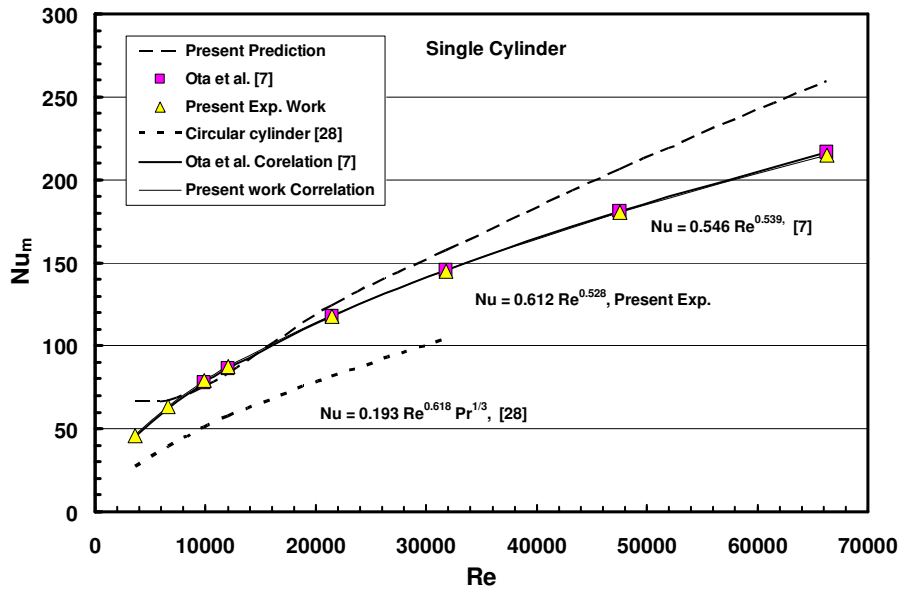


Fig. (20): Comparison of present predictions, experimental results for average Nusselt number of a single elliptic and circular cylinders without grids of [7, 8]

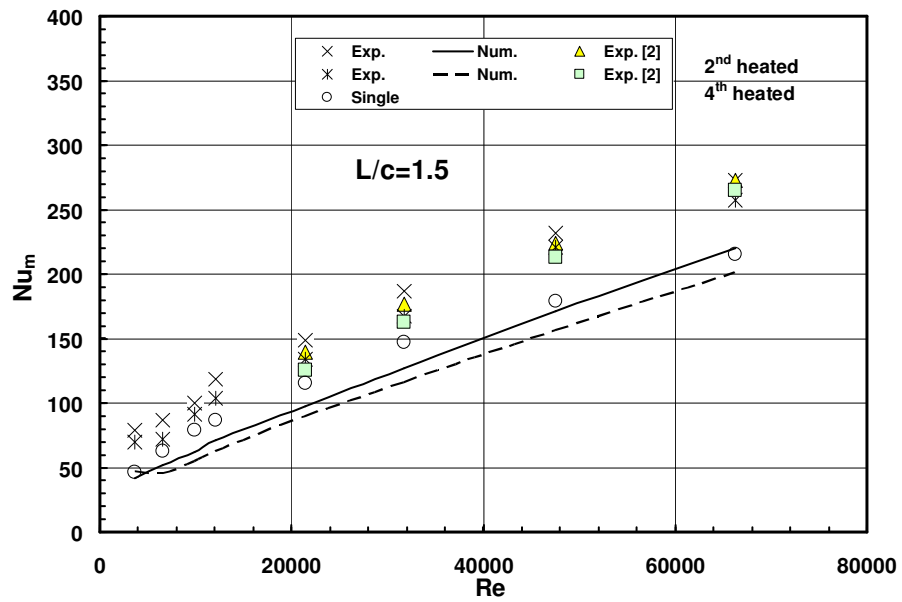


Fig. (21): Comparison of the present predictions, experimental results for the average Nusselt number with experimental results of [2] for L/c=1.5

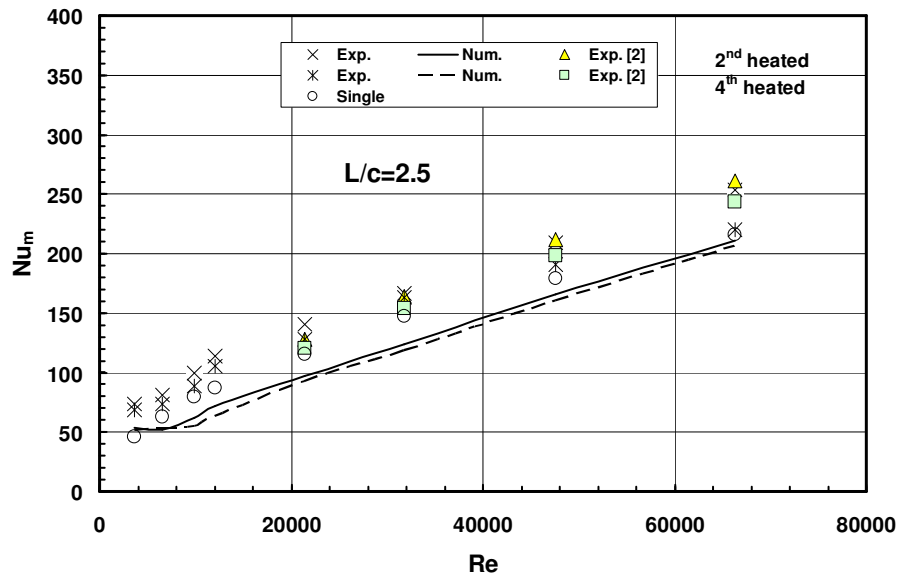


Fig. (22): Comparison of the present predictions, experimental results for the average Nusselt number with experimental results of [2] for $L/c=2.5$

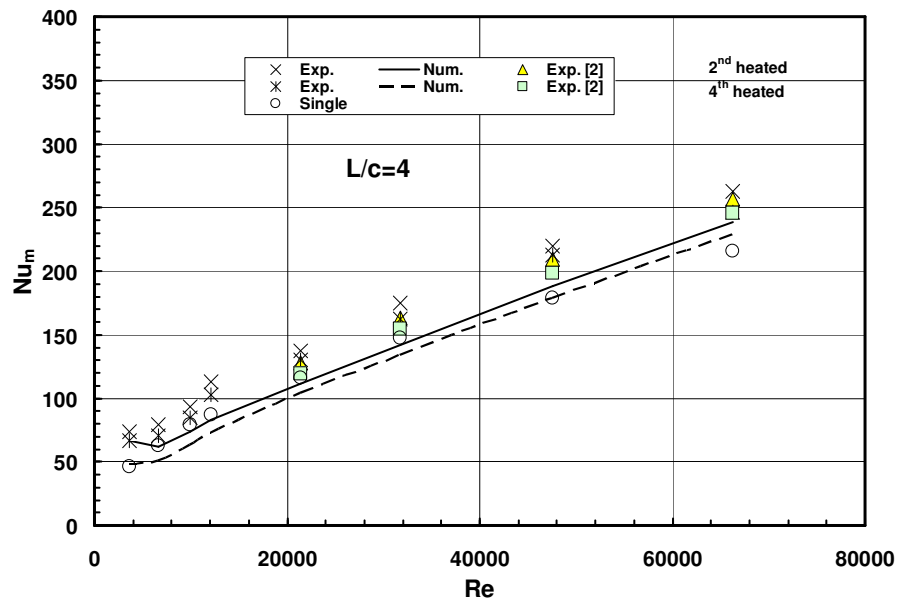


Fig. (23): Comparison of the present predictions, experimental results for the average Nusselt number with experimental results of [2] for $L/c=4$

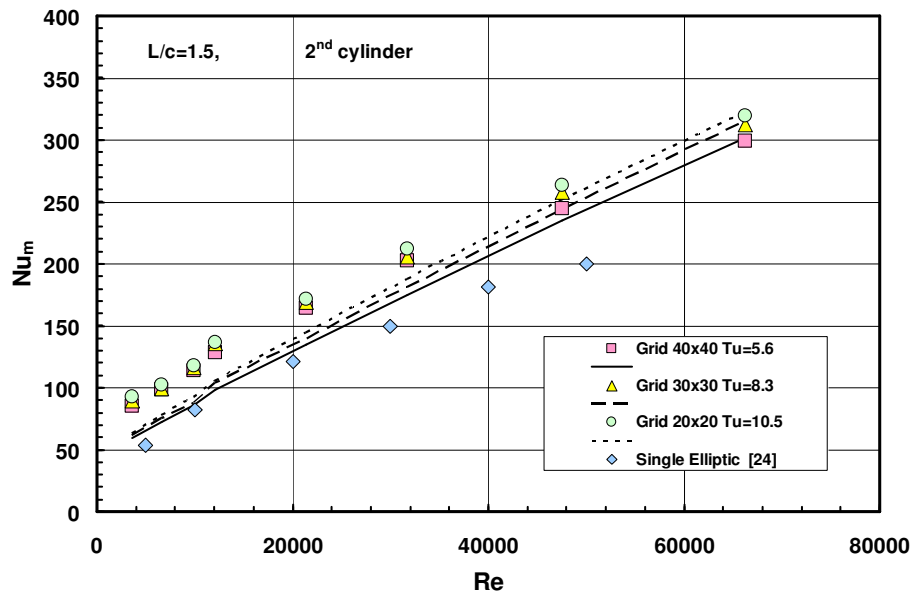


Fig. (24): Variation of the average Nusselt number versus Reynolds number for the second cylinder, $L/c=1.5$ at different grid size (experimental results and present predictions)

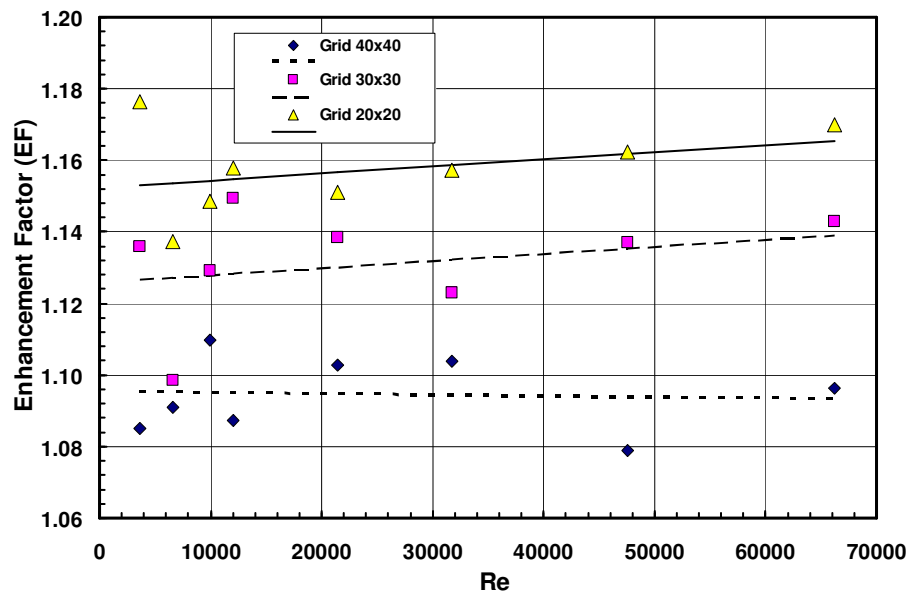
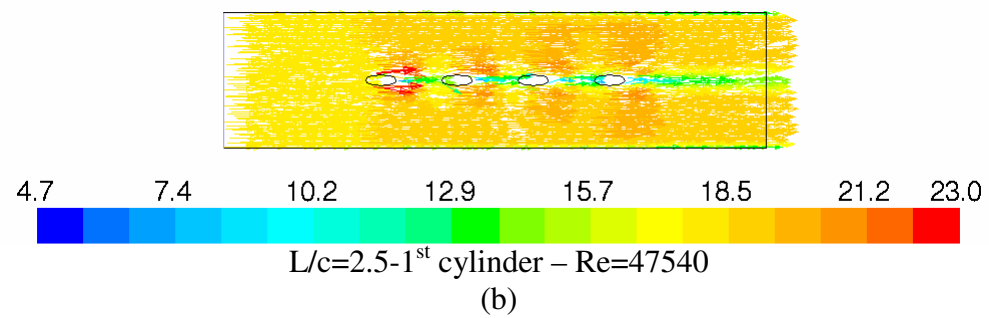
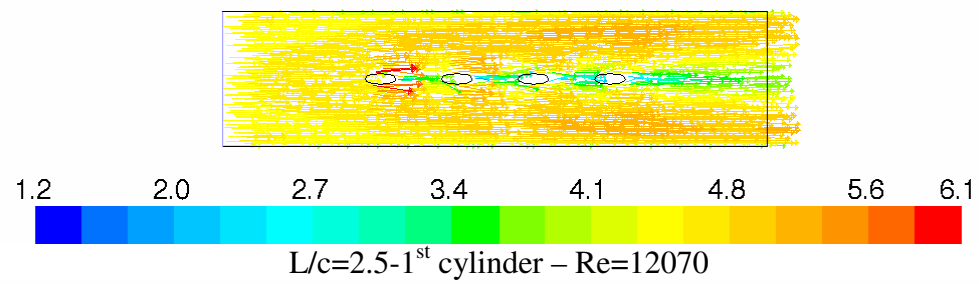
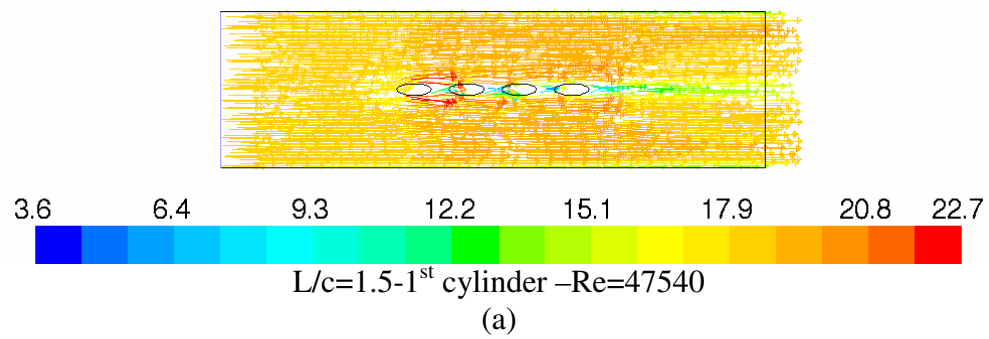
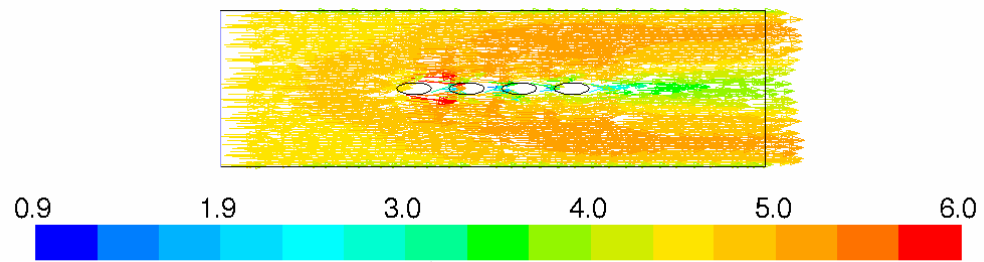


Fig. (25): Variation of the enhancement factor versus Reynolds number for the second cylinder, $L/c=1.5$ at different grid size



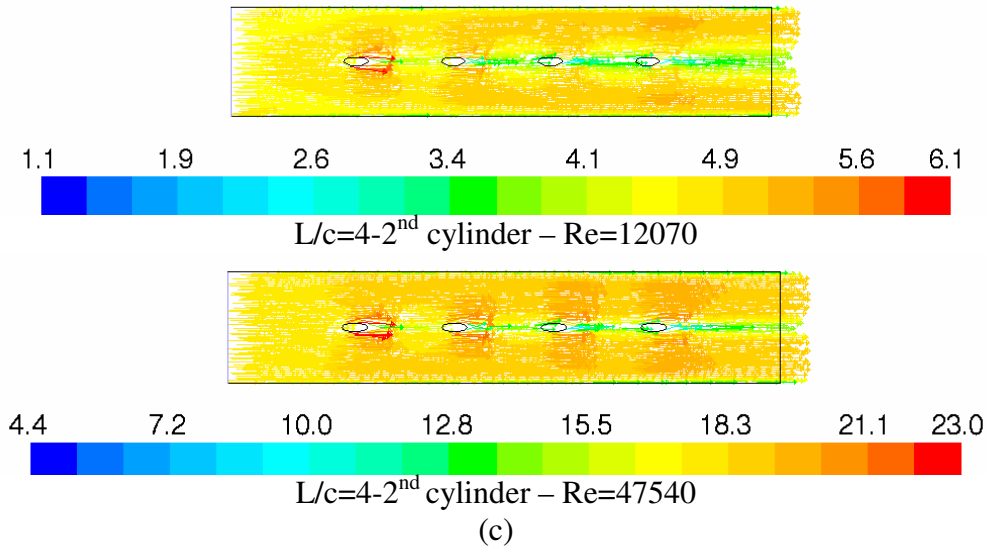


Fig. (26) Velocity vector for different spacing ratios at $Re=12070$ and $Re=47540$

5. CONCLUSIONS

Effect of free stream turbulence intensity on heat transfer and flow characteristics around four in-line elliptic cylinders in cross flow was experimentally and numerically investigated. The elliptic cylinders examined were heated under constant heat flux condition within Reynolds number (based on free stream velocity and major axis length) ranged from 3640 to 66250. The experimental runs were carried out at different cylinder spacing ratios (L/c) for three different free stream turbulence intensities levels of 5.6%, 8.3% and 10.5%. From the above discussion, the following points can be concluded:

1. It is found that the local Nusselt number distribution for the first cylinder shows no essential variation with the cylinder spacing.
2. The local Nusselt number reaches a minimum value close to $S/c=\pm 0.7$ independently of Reynolds number. Then reaches a nearly constant value up to $S/c=\pm 1.1$ for $Re \leq 21420$. At high Reynolds number ($Re \geq 31750$), the local Nusselt number begins to increase slightly downstream of the position of $S/c=\pm 0.8$.
3. The local Nusselt number is significantly increased with increasing the free stream turbulence intensities.
4. The average Nusselt number for the single elliptic cylinder, $Nu_{s,m}$, is correlated within Reynolds number, $Re=U_0c/v$, ranged from 3640 to 66250 and the following correlation is obtained:

$$Nu_{s,m} = 0.612 Re^{0.528}$$

5. It is found that the average Nusselt number for the second cylinder is higher than that of the other tested cylinder for all tested spacing ratios.
6. It is concluded that, the maximum enhancement ratio for the average Nusselt number (average Nusselt number of the tested cylinder with grid/ average Nusselt number of a single elliptic cylinder without grid) is found to be about 1.93, and is obtained for the second elliptic cylinder in four in-line cylinders at $L/c=1.5$, $Re=6150$ with free stream turbulence intensity of 10.5%.
7. It is found that the heat transfer enhancement (Nu_m with grids / Nu_m without grid) is about 10%, 14% and 16% for free stream turbulence of 5.6%, 8.3%, and 10.5% respectively.
8. Empirical correlation for the average Nusselt number of the second elliptic cylinder of four in-line cylinders is obtained as function of Reynolds number, and free stream turbulence intensity, and the following correlation is obtained:

$$Nu_m = 1.73 Re^{0.445} Tu^{0.089}$$

NOMENCLATURE

- b minor axis length of elliptic cylinder, m
- c major axis length of elliptic cylinder, m
- EF enhancement factor, $Nu_{m, \text{with grid}}/Nu_{m, \text{without grid}}$
- H duct height, m
- h local heat transfer coefficient, $W/m^2 \cdot ^\circ C$
- h_m average heat transfer coefficient to air stream, $W/m^2 \cdot ^\circ C$
- K fluid thermal conductivity, $W/m \cdot ^\circ C$
- k turbulent kinetic energy, m^2/s^2 or J/kg
- L longitudinal spacing distance, (longitudinal distance between two cylinder centers), m
- Nu local Nusselt number
- Nu_m average Nusselt number around the tested elliptic cylinder
- $Nu_{s,m}$ average Nusselt number around a single elliptic cylinder
- q_w net heat flux, W/m^2
- Re Reynolds number = $U_o c / \nu$
- S surface distance from the leading edge, taken as positive along the upper side, m
- T local surface temperature, $^\circ C$
- T_o average inlet air temperature, $^\circ C$
- Tu relative turbulence intensity, %
- u stream-wise velocity component, m/s
- U_o upstream mean velocity, m/s
- v transverse velocity component, m/s
- x stream-wise coordinate, m

y normal coordinate, m
 ε rate of dissipation of turbulent kinetic energy
 ν kinematic viscosity, m^2/s
 μ_t turbulent dynamic viscosity, $N.s/m^2$
 ρ density, kg/m^3

Subscripts

b bulk
o upstream flow
s single cylinder
w wall
x local distance in the axial direction

REFERENCES

1. Nishiyama, H., Ota, T. and Matsuno, T., "Forced convection heat transfer from two elliptic cylinders in a tandem arrangement," Trans. JSME, Vol. 52, Ser. B, pp. 2677-2681, 1986.
2. Nishiyama, H., Ota, T. and Matsuno, T., "Heat transfer and flow around elliptic cylinders in tandem arrangement," JSME International Journal, Series II, Vol. 31, No. 3, pp. 410-419, 1988.
3. Badr, H.M., "Mixed convection from a straight isothermal tube of elliptic cross section," Int. J. Heat Mass Transfer, Vol. 37, No. 15, pp. 2343-2365, 1994.
4. Abdel Aziz, A.A., Berbish, N.S., and Hanafi, A.S., "Flow and heat transfer characteristics around a combination of elliptic cylinders in-line," Eighth Int. Congress of Fluid Dynamics & Propulsion, Sharm El-sheikh, Sinai, Egypt, ICFDP8- EG-166, December 14-17, 2006.
5. Seban, R., and Drake, R., "Local heat transfer coefficients on the surface of elliptic cylinder in a high speed air stream," Trans. ASME, Vol. 75, pp. 235-240, 1953.
6. Drake, R., Seban, R., Doughty, D. and Lin, S. "Local heat transfer coefficients on the surface of elliptic cylinder, axis ratio 1:3, in a high speed air stream," Trans. ASME, Vol. 75, pp. 1291-1302, 1953.
7. Ota, T., Nishiyama, H., and Taoka, Y., "Heat transfer and flow around an elliptic cylinder," Int. J. Heat Mass Transfer, Vol. 27, No. 10, pp. 1771-1779, 1984.
8. Badr, H.M., "Forced convection from a straight elliptical tube," Int. J. Heat Mass Transfer, Vol. 34, pp. 229-236, 1998.

9. Khan, M.G., Fartaj, A. and Ting, D.S.-K., "An experimental characterization of cross-flow cooling of air via an in-line elliptical tube array," *International Journal of Heat and Fluid Flow*, Vol. 25, pp. 1-13, 2004.
10. Abdel Aziz, A.A., Berbish, N.S., and Hanafi, A.S., "Forced convection heat transfer and flow around three staggered elliptic cylinders in cross flow," *Engineering Research Journal*, Helwan University, Faculty of Engineering, Mataria, Cairo, Vol. 109, pp. M118-136, February 2007.
11. Berbish, N.S., "Heat transfer characteristics and flow behavior around four elliptic cylinders in staggered arrangement," *Scientific Bulletin*, Ain Shams Uni., Faculty of Engineering, Cairo, Egypt, Vol. 42, pp. 1119-1141, Sept. 2007.
12. Kondjoyan, A., Peneau, F. and Boisson, H., "Effect of high turbulence on heat transfer between plates and air flows; A review for existing experimental results," *Int. J. Therm. Sci.*, Vol. 41, pp. 1-16, 2002.
13. Seban, R.A., "The influence of free stream turbulence on the local heat transfer from cylinders, " *J. Heat Transfer*, Trans. ASME, Vol. 82, pp. 101-107, 1960.
14. Morgan, V.T., "The overall convective heat transfer from smooth circular cylinders," *Advances in Heat Transfer*, Vol. 11, pp. 199-264, 1975.
15. Dyban, E.P., and Epick, E. Ya., "Some heat transfer features in the air flow of intensified turbulence," *Proc. 4th Heat Transfer Conf. F.C.5.7*, Paris-Versailles, Vol. 2, 1970.
16. Dyban, E.P., Epick, E. Ya., and Kozlova, L.G. "Combined influence of turbulence intensity and longitudinal scale and air flow acceleration on heat transfer of circular cylinder," *Proc. 5th Heat Transfer Conf. F.C.8.4*, Tokyo, pp. 310-314, 1974.
17. Lowery, G.W., and Vachon, R.I., "The effect of turbulence on heat transfer from heated cylinders," *Int. J. Heat Mass Transfer*, Vol. 18, pp. 1229-1242, 1975.
18. Simmons, S.G., Hager, J.M. and Diller, T.E., "Simultaneous measurements of time-resolved surface heat flux and free stream turbulence at the stagnation point," *Proc. Of 9th Int. Heat Transfer Conf.*, Vol. 2, Hemisphere, Washington, D.C., pp. 375-380, 1990.
19. Ching, C.Y., and O' Brien, J.E., "Unsteady heat flux in a cylinder stagnation region with high free stream turbulence," *Fund. Exp. Meas. In Heat Transfer*, ASME HTD, Vol. 179, pp. 57-66, 1991.
20. Huang, C.K., Cheng, Y.J., Kang, Y.P., "Combined effect of grid turbulence and unsteady wake on convective heat transfer around a heated cylinder," *Int. J. Heat Mass Transfer*, Vol. 34, pp. 1091-1100, 2007.

21. Terekhov, V.I., Yarygina, N.I., and Zhdanov, R.F., "Heat transfer in turbulent separated flows in the presence of high stream turbulence," *Int. J. Heat Mass Transfer*, Vol. 46, pp. 4535-4551, 2003.
22. Sak, C., Lui, R., Ting, D.S.-K., and Rankin, G.W., "The role of turbulence scale and turbulence intensity on forced convection from a heated horizontal circular cylinder," *J. Experimental Thermal and fluid Science*, Vol. 31, pp. 279-289, 2007.
23. Choi, J., Teng, S. Han, J. and Ladeinde, F., "Effect of free stream turbulence on turbine blade heat transfer and pressure coefficients in low Reynolds number flows," *Int. J. Heat Mass Transfer*, Vol. 47, pp. 3441-3452, 2004.
24. Kondjoyan, A. and Daudin, J.D., "Effects of free stream turbulence intensity on heat and mass transfers at the surface of a circular cylinder and an elliptical cylinder, axis ratio 1:4," *Int. J. Heat Mass Transfer*, Vol. 38, No. 10, pp. 1735-1749, 1995.
25. Scholten, J.W. and Murray, D.B., "Unsteady heat transfer and velocity of a cylinder in cross flow – I. Low free stream turbulence," *Int. J. Heat Mass Transfer*, Vol. 41, No. 10, pp. 1139-1148, 1998.
26. Scholten, J.W. and Murray, D.B., "Unsteady heat transfer and velocity of a cylinder in cross flow – II. High free stream turbulence," *Int. J. Heat Mass Transfer*, Vol. 41, No. 10, pp. 1149-1156, 1998.
27. Ahmed, E. H., and Badr, H.M., "Mixed convection from an elliptic tube placed in a fluctuating free stream," *Int. J. of Engineering Science*, Vol. 39, pp. 669-693, 2001.
28. *Fluent Version 6.2 User's Guide*, Fluent Incorporated, New Hampshire, 2001.
29. Cengel, Y.A., *Heat Transfer: A practical Approach*, McGraw-Hill, Boston, Massachusetts, 1998.